ELSEVIER

Journal of Nuclear Materials 252 (1998) 121–130

journal of nuclear materials

# Mechanistic interpretations of $UO_2$ oxidation

D.R. Olander *

*Department of Nuclear Engineering, University of California, Berkeley, CA 94720, USA*

Received 7 March 1997; accepted 2 September 1997

**Abstract**

The literature dealing with experiments and modeling of $UO_2$ oxidation at temperatures $> \sim 600$°C is reviewed and a detailed model is proposed. Mechanistic modeling is subjected to the principle of detailed balancing, which provides a framework for the elementary reactions contained in the reaction scheme. This principle interrelates the rate constants of the model, provides a link to gas–solid thermochemistry, and constrains the forms of the rate laws applied to the elementary steps of the model. Previous mechanistic models are analyzed in these terms and the rate constants deduced from them are assessed. A more general oxidation mechanism is proposed and compared to typical data. The types of new experiments needed to elucidate the mechanism are suggested. © 1998 Elsevier Science B.V.

## 1. Introduction

The effects of oxidation from $UO_2$ to $UO_{2+x}$ on the properties of light-water reactor fuel are widely recognized. The situations in which this process is important cover temperatures from 100 to 2000°C. In the 100–400°C range, addition of oxygen to spent fuel in a nuclear waste repository is the first step in formation of the higher oxides $U_4O_9$, $U_3O_7$ and $U_3O_8$ [1]. Here the principal oxidant is $O_2$ in air; moisture has a minor effect and hydrogen is not present.

Oxidation in the 450°–650°C range is a concern during normal operation of a defective fuel rod, which has become flooded with steam due to opening of a small flaw in the cladding. Here the reactive species are $H_2O$ and $H_2$, with perhaps a small but potent contribution from radiolytically-produced $O_2$ and $H_2O_2$ [2]. The presence of $H_2$ produced by steam corrosion of the inner cladding wall results in competition between fuel reduction by hydrogen and oxidation by steam and the oxidizing radiolysis products. In defective fuel rods, the chief concern is the hydrogen produced by fuel oxidation. This added source of $H_2$ can contribute to hydriding of the cladding.

In the upper temperature range, 1000–2000°C, fuel oxidation is an issue in severe accident analysis. Research with this objective in mind includes the work of Bittel et al. [3], Cox et al. [4], Abrefah et al. [5], and most recently, the experimental investigation of Imamura and Une [6] and the theoretical work of Dobrov et al. [7]. In addition to the well known effects of fuel oxidation on fission gas release (enhanced) and fuel thermal conductivity (reduced), the chemical states of the fission products released in the degrading core are very sensitive to the O/M ratio of the fuel. The oxidizing species in this temperature range is $H_2O$, which is diluted with $H_2$. In an air-ingress accident, $O_2$ could also be involved.

## 2. Mechanistic analysis of $UO_2$ oxidation

The earliest investigations of the reaction of water vapor with $UO_2$ dates from the last century. At the time of the Manhattan project, water vapor at 310°C was reported to have no effect on $UO_2$ [8]. In recent work on $UO_2$ oxidation by steam in the high-temperature range, Bittel et al. [3] interpreted the data in terms of kinetics controlled

* Fax: +1-510 643 9685.


*PII* S0022-3115(97)00291-2

by oxygen diffusion in the solid. However, oxygen diffusion in $UO_{2+x}$ is fast [9], and Cox et al. [4] recognized that their experimental results (and those of Bittel et al.) could only be interpreted in terms of a surface-reaction controlled process. They showed that the oxidation kinetics could be adequately described by a phenomenological rate law originally proposed by Carter and Lay [10] for the oxidation of $UO_2$ in $CO/CO_2$ gas mixtures. Based on the activation energies of the surface reaction ($\sim$ 200 kJ/mol) and oxygen chemical diffusion in $UO_{2+x}$ ($\sim$ 50 kJ/mol), solid-state oxygen diffusion is expected to control the kinetics in steam/hydrogen gases only for temperatures greater than $\sim$ 1800°C.

Given the importance of surface processes on the kinetics of $UO_2$ oxidation, a mechanistic rather than a phenomenological framework for interpreting oxidation data is clearly desirable. The purpose of the present work is to broaden the scope of existing mechanistic interpretations to provide interpretive guidance for future fuel oxidation studies that extend the database beyond the limited range of variables on which current analyses are based. The presently-available data are predominantly in atmospheric-pressure steam/hydrogen gases in the temperature range 1000–1400°C. Imamura and Une [6] have extended the temperature range down to 800°C and these authors and Olander et al. [2] have produced a few data using $H_2O_2$ as a reactant gas.

### 2.1. Equilibrium considerations

$UO_2$ oxidation in steam–hydrogen is a classic example of an equilibrium-limited reaction; in a gas of specified $H_2O/H_2$ ratio, the reaction ceases at a fuel O/U when the oxygen potential of the gas is equal to that of the solid oxide. The oxide can be returned to $UO_2$ by switching the ambient gas to pure $H_2$, and the oxidation–reduction cycles are indefinitely reproducible [5]. Thus the kinetic analysis is closely tied to the thermochemistry of $UO_{2+x}$, which is fortunately well-established. The condition of gas–solid equilibrium is given by

$$P_{H_2O}/P_{H_2} = \sqrt{K_W P_{O_2}} = q(x), \tag{1}$$

where $P_{H_2O}$, $P_{O_2}$ and $P_{H_2}$ are the partial pressures of steam, oxygen and hydrogen, respectively (in atm) and $K_W$ is the equilibrium constant of the reaction

$$2H_2(g) + O_2(g) = 2H_2O(g) \tag{2}$$

for which the law of mass action is

$$K_W = \frac{P^2_{H_2O}}{P^2_{H_2} P_{O_2}}. \tag{3}$$

$q(x)$ in Eq. (1) is a form of the oxygen activity in $UO_{2+x}$. The fuel oxygen potential, basically $P_{O_2}$ as a function of $x$ and $T$, is given by the thermochemical models of Blackburn [11] or Lindemer and Besmann [12]. From either of these, the oxygen activity function $q(x)$ can be constructed (the temperature is omitted from the function description for simplicity), as shown in Fig. 1. Oxidation occurs when $P_{H_2O}/P_{H_2} > q(x)$ and reduction takes place when $P_{H_2O}/P_{H_2} < q(x)$. All of the experiments which have been subject to mechanistic analysis were of the former type.

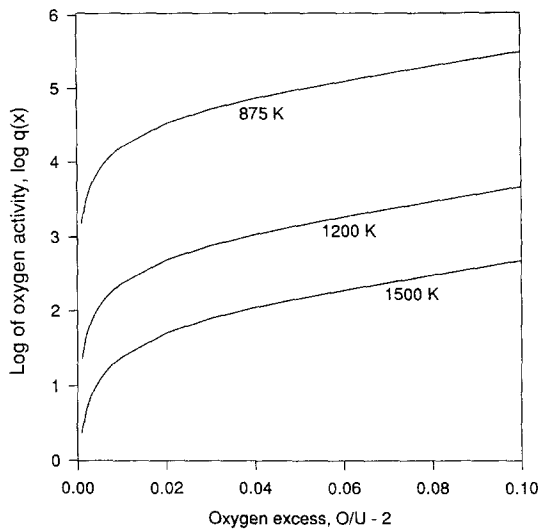


Fig. 1. Oxygen activity of $UO_{2+x}$.

### 2.2. Phenomenological model

The phenomenological description of oxidation [4,5,10] takes the form

$$\left(\frac{\rho_U V}{S}\right)\dot{x} = k_{phen}(x_{eq} - x), \tag{4}$$

where the dot refers to the time derivative. $\rho_U$ is the molar density of uranium in $UO_2$ and S/V is the surface-to-volume ratio of the specimen. $k_{phen}$ is a rate constant that depends on temperature and probably on steam pressure, but not on the $P_{H_2O}/P_{H_2}$ ratio. The latter dictates the equilibrium stoichiometry $x_{eq}$ via Eq. (1). The experimental data are in reasonable agreement with the exponential approach to equilibrium predicted by Eq. (4). This accord, which holds over a wide range of steam–hydrogen mixtures in the gas, and the one-parameter nature of the rate law have made Eq. (4) a popular tool in severe accident analyses [13].

However, Eq. (4) cannot be derived from a reaction mechanism, which is a set of elementary reactions that sum to the overall reaction

$$H_2O(g) \rightarrow H_2(g) + O(s), \tag{5}$$

where O(s) represents oxygen in the solid in excess of that contained in stoichiometric $UO_2$. Thus there is no way of extrapolating the experiments to conditions (excepting perhaps temperature) beyond those in which the data were

obtained. This deficiency of the phenomenological model is the reason for the need to develop mechanistic models.

### 2.3. Detailed balancing

The equilibrium limitation in Eq. (4) is included on an ad hoc basis, in a manner similar to the temperature difference that provides the driving force for heat transfer. However, in mechanistic models, the equilibrium condition enters in a more formal way, which is called the principle of detailed balancing [14,15]. This principle states that each elementary step in a reaction sequence must be accompanied by its reverse, and at equilibrium, the rates of the forward and reverse reactions of *all* elementary steps must be equal. This condition is more restrictive than requiring the overall reaction to cease. Detailed balancing leads to relationships between the rate constants of elementary reactions in a mechanistic scheme and also constrains the forms of the kinetic expressions that can be used to described the rates of the elementary steps.

In addition, forward and reverse reaction pairs must connect all reacting species in all phases in which the model assumes them to be present. In the case of $UO_2$ oxidation by steam–hydrogen mixtures, a small but non-zero partial pressure of oxygen is present in the gas phase by virtue of the equilibrium of Eq. (2). The molecular units are partitioned as follows: $O_2$ and $H_2$ are present only in the gas phase; $H_2O$ exists in the gas and in the surface (adsorbed) phase; and atomic O is present in the surface as an adsorbed species and in the solid as the oxygen excess. Other species such as the hydroxyl radical (OH) may be included in a reaction scheme. It has not been used in modeling of $UO_2$ oxidation by steam, but may be necessary if reaction with $H_2O_2$ is included in the mechanism.

### 2.4. Gala–Grabke model

The first mechanistic interpretation of the kinetics of steam oxidation of $UO_2$ was proposed by Abrefah et al. [5], who utilized Gala and Grabke's [16] model of FeO oxidation in steam–hydrogen mixtures as a template. Although the original mechanism proposed by Gala and Grabke contained several elementary reactions and included OH as a surface species, the adaptation of this theory by Abrefah and al was limited to the single rate-controlling step

$$H_2O(g) \leftrightarrow O(s) + H_2(g). \tag{6}$$

Although this reaction is formally identical to the overall reaction given by Eq. (5), Eq. (6) represents the sum of three elementary steps of which two are assumed to be in equilibrium. The two equilibrium elementary reactions proceed rapidly so that the above reaction appears to be an elementary process. The double-headed arrow in Eq. (6) indicates forward and reverse processes, each of which has a rate law. The rate of the forward reaction is proportional to the partial pressure of steam, and the reverse step is proportional to the partial pressure of hydrogen multiplied by a function of the oxygen excess, $f(x)$. At equilibrium, the forward and reverse rates are equal, leading to the condition

$$k_1 P_{H_2O} = f(x) P_{H_2}. \tag{7}$$

Because this is an equilibrium condition, Eq. (1) applies, so that Eq. (7) provides a relation between the function $f(x)$ and the oxygen activity $q(x)$:

$$f(x) = k_1 q(x). \tag{8}$$

The kinetic equation during oxidation is

$$\left(\frac{\rho_U V}{S}\right)\dot{x} = k_1 P_{H_2O} - f(x) P_{H_2} = k_1 P_{H_2O} - k_1 q(x) P_{H_2}$$
$$= k_1 P_{H_2O}(1 - B), \tag{9}$$

where $f(x)$ has been replaced using Eq. (8) and the thermodynamic factor is defined by

$$B = \frac{q(x)}{P_{H_2O}/P_{H_2}}. \tag{10}$$

At the start of oxidation, when $x \sim 0$, the factor $B$ is $\ll 1$. At equilibrium, $B = 1$ and the reaction stops.

To this point, the Gala–Grabke treatment is mechanistic. However, to fit the model to FeO oxidation data, these authors, as well as Abrefah et al. [5], found it necessary to allow the rate constant $k_1$ to be a function of fuel oxygen activity. The empirical form chosen was

$$k_1 = k_1^+ / [q(x)]^n, \tag{11}$$

where the rate constant $k_1^+$ is a function of temperature only and $n$ is a constant.

The Gala–Grabke model, and its application to $UO_2$ oxidation by Abrefah et al. [5] has two shortcomings. The first is the empirical fuel stoichiometry factor in the rate constant expressed by the $q(x)^n$ term in Eq. (11). The second is the inability of the model to correctly predict the steam–pressure dependence of the oxidation rate; Eq. (9) predicts a linear dependence of the rate on $P_{H_2O}$ while the data show a square-root variation of the rate of oxidation with steam partial pressure.

### 2.5. The model of Dobrov et al.

In order to rectify the failure of the Gala–Grabke model to correctly predict the steam–pressure dependence of the rate of $UO_2$ oxidation in steam–hydrogen gases, Dobrov et al. [7] included a water-adsorption step in the mechanism. They also included elementary steps involving adsorbed atomic oxygen, but these processes are superfluous in the development of the final rate equation. Without these, the Dobrov model is contained in the following elementary steps:

$$H_2O(g) \leftrightarrow H_2O(ads) \tag{12}$$

$$H_2O(ads) \leftrightarrow O(s) + H_2(g), \tag{13}$$

where $H_2O$(ads) represents water adsorbed on the surface of the oxide. The forward step of reaction (12) is given by the Hertz–Langmuir equation for the flux of $H_2O$ to the surface multiplied by the fraction of the surface that is not occupied by $H_2O$(ads). This assumption is the basis of the Langmuir adsorption isotherm in physical adsorption. The reverse step in Eq. (12) is proportional to the surface concentration of $H_2O$(ads), with the rate constant denoted by $k_a$. The forward step of reaction (13) proceeds with a rate constant $k'_a$ and the rate constant of the reverse process is determined by applying the principle of detailed balancing. At equilibrium, the forward and reverse rates of Eqs. (12) and (13) must be equal, leading to

$$\frac{\beta_{H_2O} P_{H_2O}}{n_S}\left(1-\theta_{H_2O}\right) = k_a \theta_{H_2O} \tag{14}$$

$$k'_a \theta_{H_2O} = \frac{f(x) P_{H_2}}{n_S}\left(1-\theta_{H_2O}\right), \tag{15}$$

where $\theta_{H_2O}$ is the fraction of the solid surface occupied by $H_2O$(ads) (i.e., the coverage) and $n_S$ is the density of adsorption sites on the surface. The water adsorption rate at 1 atm steam pressure is

$$\beta_{H_2O} = s\left(2\pi RTM_{H_2O}\right)^{-1/2}, \tag{16}$$

where $R$ is the gas constant, $T$ is the temperature, and $M_{H_2O}$ is the molecular weight of water. $s$ is the sticking probability, or the fraction of water molecules striking the bare $UO_2$ surface that is adsorbed.

The stoichiometry-dependent rate constant for the reverse step of Eq. (13) is determined by dividing Eqs. (14) and (15) and using Eq. (1):

$$f(x) = \beta_{H_2O} \frac{k'_a}{k_a} q(x). \tag{17}$$

The non-equilibrium balance equations on $H_2O$(ads) and O(s) are

$$\dot{\theta}_{H_2O} = \frac{\beta_{H_2O} P_{H_2O}}{n_S}\left(1-\theta_{H_2O}\right) - \left(k_a + k'_a\right)\theta_{H_2O} + \frac{\beta_{H_2O} P_{H_2}}{n_S}\frac{k'_a}{k_a}\left(1-\theta_{H_2O}\right) q(x), \tag{18}$$

$$\left(\frac{\rho_U V}{S}\right)\dot{x} = n_S k'_a \theta_{H_2O} - \frac{k'_a}{k_a}\beta_{H_2O} P_{H_2}\left(1-\theta_{H_2O}\right) q(x). \tag{19}$$

In applying the above equations to $UO_2$ oxidation, the quasi-stationary approximation $\dot{\theta}_{H_2O} \approx 0$ is reasonable because the surface layer has a negligible capacity to store oxygen compared to the bulk solid. This assumption permits Eq. (18) to be solved for the surface coverage of $H_2O$(ads):

$$\theta_{H_2O} = \frac{AP_{H_2O}}{1 + AP_{H_2O}}, \tag{20}$$

where

$$A = \frac{\beta_{H_2O}/n_S}{k_a + k'_a}\left(1 + \frac{k'_a}{k_a} B\right) \tag{21}$$

and B is the thermodynamic factor given by Eq. (10). Eq. (20) is the Langmuir isotherm. Substituting Eqs. (20) and (21) into Eq. (19) gives the final rate equation:

$$\left(\frac{\rho_U V}{S}\right)\dot{x} = n_S k'_a \frac{AP_{H_2O}}{1 + AP_{H_2O}} \frac{1-B}{\left(1 + \left(k'_a/k_a\right)B\right)}. \tag{22}$$

In the result obtained by Dobrov et al. [7], the parenthetical terms in Eqs. (21) and (22) are unity. Using this abbreviated formula, these authors fitted the existing steam-oxidation data with the two parameters of the model, the product $n_S k'_a$ and the water-adsorption coefficient A. The latter was found to be temperature-independent and equal to 2.5 $atm^{-1}$. Using the typical monolayer coverage $n_S = 10^{14}$ molecules/$cm^2$ or $2 \times 10^{-10}$ moles/$cm^2$, $k'_a$ is $\sim 60\ s^{-1}$ at 1300 K and $\sim 3000\ s^{-1}$ at 1700 K. Taking a mean temperature of 1500 K and assuming unit sticking probability, the $H_2O$ adsorption rate factor from Eq. (16) is $\beta_{H_2O} \sim 0.3$ mol $cm^{-2}\ s^{-1}\ atm^{-1}$. Using these numbers in Eq. (21) gives a temperature-independent value of the water desorption rate constant of $k_a \sim 5 \times 10^8\ s^{-1}$. Since $k'_a \ll k_a$, Dobrov et al.'s neglect of the parenthetical correction factors in Eqs. (21) and (22) is justified ex post facto.

The model of Dobrov et al. fits the existing data reasonably well, particularly those sets in which the steam pressure was less than 1 atm. On data-fitting grounds, this model is quite successful. However, a model that is constructed from elementary chemical or physical processes must produce rate constants that are consistent with the processes represented. Here, the consequences of the Dobrov model are less satisfying. In particular, the finding of zero activation energy for the rate constant $k_a$ and the assumption of unit sticking probability of water on the surface of $UO_2$ are not consistent with what is known of these basically physical processes.

In one-atmosphere steam at all temperatures between 1300 K and 1700 K, Eq. (20) predicts a $\sim 70\%$ coverage of the $UO_2$ surface with $H_2O$(ads). Such a high coverage cannot be sustained at these temperatures without strong binding of $H_2O$ to the solid surface. The rate constant for simple desorption of a surface-bound species without chemical change is of the form [17,18]

$$k_a = \nu e^{-\Delta H_{ads}/RT}, \tag{23}$$

where $\nu \sim 10^{13}\ s^{-1}$ is the vibration frequency of the adsorbed molecule normal to the surface and $\Delta H_{ads}$ is the heat of adsorption of $H_2O$ on the surface (i.e., the binding energy). It is physically unrealistic that the binding energy be zero; if it were, water molecules could not interact with the $UO_2$ surface in the manner assumed in the model because a significant population of $H_2O$(ads) could not be sustained. In addition, the pre-exponential factor of $k_a$

deduced from the data is 4–5 orders of magnitude smaller than expected. Deviations from the typical value of $10^{13}$ are common, but they are usually less than one or at most two orders of magnitude. Thus the pre-exponential factor and the activation energy of the rate constant for water desorption deduced by Dobrov et al. are at odds with physically-acceptable values of these parameters.

Although the sticking probability of diatomic molecules on metal surfaces can approach unity, non-dissociative adsorption on non-metal surfaces can be much lower [17]. If instead of a value of unity, the sticking coefficient of $H_2O$ on $UO_2$ were several orders of magnitude lower, so too would be the value of $\beta_{H_2O}$ and ultimately, the value of the pre-exponential factor of $k_a$ deduced from the oxidation rate data.

The shortcoming of the Dobrov model when tested against the criterion of reasonableness of the deduced parameters of the elementary steps suggests that this mechanism may not be appropriate, or at least not complete.

Lewis [19] has suggested a means of dealing with the difficulty of the lack of temperature variation of the desorption rate constant $k_a$. For the case $k'_a \ll k_a$, Eqs. (21) and (22) reduce to

$$\left(\frac{\rho_U V}{n_S S}\right)\dot{x} = k'_a \frac{AP_{H_2O}}{1 + AP_{H_2O}}(1 - B), \tag{22a}$$

where

$$A = \frac{\beta_{H_2O}}{n_s k_a}. \tag{21a}$$

The coefficient of the $1 - B$ term was fitted by Dobrov et al. using a constant value of $A$ and placing all of the temperature effect on $k'_a$. Lewis showed that a thermally-activated desorption rate constant of the form given by Eq. (23) combined with a surface reaction rate constant

$$k'_a = \nu'_a e^{-E'_a/RT}$$

with parameters different from those given by Dobrov et al. also provides acceptable agreement with the data. In particular, Lewis set $\nu = 10^{13}$ s$^{-1}$ and $\Delta H_{ads} = 40$ kcal/mol in $k_a$ and determined the parameters in $k'_a$ that provided the best agreement with the combination $k'_a A/(1 + A)$ found by Dobrov et al. to best fit the ensemble of the experimental results. The parameters of $k'_a$ determined by Lewis in this manner are $\nu'_a = 4 \times 10^{10}$ s$^{-1}$ and $E'_a = 54$ kcal/mol. Comparison of Dobrov's combined kinetic parameter determined from the database and Lewis' counterpart determined using Dobrov's results as 'data' is shown in Fig. 2. The agreement between the two combined kinetic parameter curves is within 20%, but this does not imply comparable agreement of Lewis' modified theory with the original data. Moreover, the pressure dependence of the oxidation rate in Lewis model depends on temperature. At high temperature $k_a$ is large, $A$ is small, and the pressure dependence of Eq. (22a) approaches linearity. At low temperature, Lewis's theory predicts little temperature dependence. Not enough data are available to verify this distinction. Finally, use of a thermally-activated $k_a$, however desirable from a physical point of view, adds another parameter to be determined from a data set that is barely able to provide accurate values of the rate constants in Dobrov's three-parameter theory.

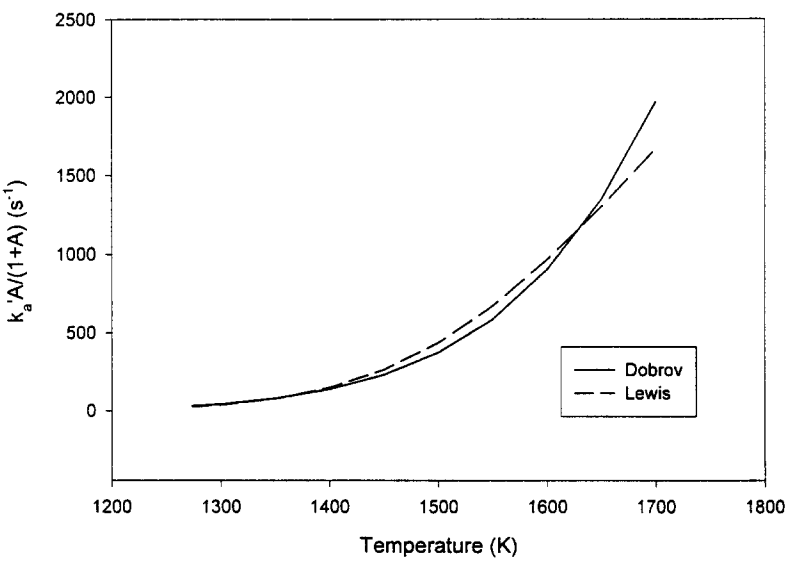


Fig. 2. Comparison of Dobrov's and Lewis' fits of the pressure- and temperature-dependent rate constant combination at a steam pressure of 1 atm.

### 2.6. An extended $UO_2$ oxidation / reduction model

The purpose of this section is to present a model of $UO_2$ oxidation and $UO_{2+x}$ reduction that is intended to serve as a framework for interpreting future experimental results. No attempt is made to fit the extended model to existing data, which are too sparse to be fitted to any model that has more than two rate constants. The current mechanistic models (Sections 2.4 and 2.5) adequately reproduce the results of currently-available experiments, and even the single-parameter phenomenological representation (Section 2.3) is sufficient for this purpose. The proposed model is sufficiently general to apply to a variety of reactant gas mixtures ($H_2O/H_2$, $H_2$/inert, $H_2O/O_2$, $H_2O$/inert, and $O_2$/inert) at total pressures other than 1 atm. The existing experimental database covers only the first two of these gas combinations and is restricted to a total pressure of 1 atm and temperatures from ~1000 to 1400°C.

The extended model is based on the mechanism proposed by Dobrov et al. [7], but more fully utilizes elementary steps and species (O(ads)) contained in the latter but not exploited in its development. The extended model consists of the following set of forward and reverse pairs:

$$H_2O(g) \leftrightarrow H_2O(ads) \tag{24}$$

$$H_2O(ads) \leftrightarrow H_2(g) + O(ads) \tag{25}$$

$$O_2(g) \leftrightarrow 2O(ads) \tag{26}$$

$$O(ads) \leftrightarrow O(s). \tag{27}$$

Reaction (26) must be included in the model even though the partial pressure of $O_2$ in the gas may be very low. The reason is that Eq. (2), which contains $O_2$, is an integral part of the model. The mechanism of Dobrov et al. neglects Eq. (26) and combines Eqs. (25) and (27) into Eq. (13).

#### 2.6.1. Equilibrium

When the system is at equilibrium, all steps are individually at equilibrium (principle of detailed balancing), which leads to the following equations:

$$\frac{\beta_{H_2O} P_{H_2O}}{n_S}\left(1 - \theta_O - \theta_{H_2O}\right) = k_a \theta_{H_2O}, \tag{28}$$

$$k''_a \theta_{H_2O} = k P_{H_2} \theta_O, \tag{29}$$

$$\frac{\beta_{O_2} P_{O_2}}{n_S}\left(1 - \theta_O - \theta_{H_2O}\right)^2 = k_d n_S \theta_O^2, \tag{30}$$

$$k_S \theta_O = k'_S\left(1 - \theta_O - \theta_{H_2O}\right) f(x), \tag{31}$$

where

$$\beta_i = \frac{s_i}{\sqrt{2\pi M_i RT}}. \tag{32}$$

In Eq. (29), $k$ is the rate constant for the reverse step of reaction (25), and $k_d$ in Eq. (30) is the rate constant for associative desorption of O(ads). In Eq. (31), $k_S$ is the rate constant governing incorporation of O(ads) into the solid. $s_i$ is the sticking probability of species $i$ on the bare(uncovered) $UO_2$ surface [17]. The function $f(x)$ describes the stoichiometry-dependence of the reverse step of reaction pair given by Eq. (27). The coverage factor in the parentheses of Eq. (31) accounts for the requirement of an empty site for transfer of an O atom from the solid to the surface. $n_S$ is the density of adsorption sites on the surface and $\theta_i$ is the fraction of the sites occupied by species $i$. Langmuir adsorption is assumed for both $H_2O$ and $O_2$. However, since $O_2$ adsorption is dissociative, two adjacent sites must be empty; the coverage dependence of the adsorption rate of this species depends on the square of the fraction of unoccupied sites [17]. The units of the rate constants are: $\beta$: mol $s^{-1}$ $cm^{-2}$ $atm^{-1}$; $k_a$ and $k''_a$: $s^{-1}$; $n_S$: mol $cm^{-2}$; $k$: $s^{-1}$ $atm^{-1}$; $k_d$: $cm^2$ $mol^{-1}$ $s^{-1}$; $k_S$ and $k'_S$: $s^{-1}$.

The equilibrium must also satisfy the thermochemistry of $UO_{2+x}$, which is expressed by Eq. (1). The gas phase is assumed to be in chemical equilibrium, so that the partial pressures of $H_2$, $O_2$ and $H_2O$ are related by Eq. (3).

Eqs. (28)–(31) are solved as follows: Eliminating $\theta_{H_2O}$ and $\theta_O$ between Eqs. (28)–(30) and using Eq. (3) for $P_{O_2}$ yields the following relation between the rate constants:

$$\frac{\beta_{H_2O}}{\sqrt{\beta_{O_2}}} \frac{k''_a \sqrt{K_W k_d}}{k_a k} = 1. \tag{33}$$

Eliminating $\theta_{H_2O}$ and $\theta_O$ using Eqs. (30) and (31) and expressing $P_{O_2}$ by Eq. (1) results in

$$f(x) = E(k_S/k'_S) q(x), \tag{34}$$

where $E$ is the dimensionless group:

$$E = \left(\frac{\beta_{O_2}}{K_W k_d n_S^2}\right)^{1/2} = \frac{\beta_{H_2O} k''_a}{k_a k n_S}. \tag{35}$$

The second equality in the above equation results from use of Eq. (33).

Eqs. (33)–(35) contain only kinetic constants and thermochemical properties; they do not (and must not) involve the partial pressures of the reactant gases. Satisfying this requirement places constraints on the forms of the individual rate expressions. For example, the coverage term in parentheses in Eqs. (30) and (31) must appear as shown in order to obtain rate-constant relationships in which gas partial pressures are absent.

#### 2.6.2. Non-equilibrium rate equations

During oxidation of $UO_2$, some or all of the elementary steps Eqs. (24)–(27) may not be in equilibrium. In place of Eqs. (28)–(31), the following balance equations for O(ads), $H_2O$(ads), and O(solid) apply:

$$\dot{\theta}_O = \frac{2\beta_{O_2} P_{O_2}}{n_S}\left(1 - \theta_O - \theta_{H_2O}\right)^2 - 2k_d n_S \theta_O^2 + k''_a \theta_{H_2O} - k\theta_O P_{H_2} - k_S\left[\theta_O - E\left(1 - \theta_O - \theta_{H_2O}\right) q(x)\right] \cong 0, \tag{36}$$

$$\dot{\theta}_{H_2O} = \frac{\beta_{H_2O} P_{H_2O}}{n_S}\left(1 - \theta_O - \theta_{H_2O}\right) - \left(k_a + k_a''\right)\theta_{H_2O} + k\theta_O P_{H_2} \cong 0, \quad (37)$$

$$\left(\rho_U V n_S S\right)\dot{x} = k_s\left[\theta_O - E\left(1 - \theta_O - \theta_{H_2O}\right) q(x)\right]. \quad (38)$$

Eq. (34) has been used to express the transfer rate of oxygen from the solid to the surface and the rate constants in Eqs. (36) and (37) must satisfy the constraint of Eq. (33). The quasi-stationary approximation has been applied to the surface coverages of $H_2O$(ads) and O(ads). In Eq. (36), $P_{O_2}$ is given in terms of $P_{H_2O}$ and $P_{H_2}$ by Eq. (3). In $H_2O/H_2$ reactant gases, the latter two pressures are specified constants and $P_{O_2}$ is eliminated using Eq. (3). However, most of the experimental work has been conducted in pure steam, for which the stoichiometry of Eq. (2) requires that $P_{H_2} = 2P_{O_2}$. Eq. (3) then yields

$$P_{O_2} = \left(\frac{P_{H_2O}^2}{4K_W}\right)^{1/3}. \quad (39)$$

As algebraic equations, Eqs. (36) and (37) can be solved simultaneously for $\theta_O$ and $\theta_{H_2O}$ in terms of the hydrogen and steam pressures and the current stoichiometry $x$. These surface coverages are then used in Eq. (38) for integrating this equation. The thermodynamic limit to the oxidation rate given by Eq. (38) cannot be expressed in terms of the simple $1 - B$ factor as in Eqs. (9) and (22). Nevertheless, in $H_2O/H_2$ gases, the rate of oxidation becomes zero as $B$ approaches unity.

### 2.6.3. Comparison with experiment

Considerable simplification is achieved by recognizing the magnitudes of the rate constants in Eqs. (36)–(38). At temperatures greater than about 1000°C, purely surface reactions such as those described by Eqs. (24)–(26) generally occur on time scales of milliseconds or less. They are studied by modulated molecular beam experiments, in which a beam of reactant gas is chopped by a rotating disk at frequencies from 100 to 1000 Hz prior to striking the solid surface where reaction takes place [20]. Reaction products leave the surface with the same modulation frequency and are measured by phase-lock detection techniques. This type of surface chemical reaction analysis is possible because the characteristic reaction times match the modulation frequencies. The modulated molecular beam method has been applied to surface reactions involving $UO_2$ [21,22].

The surface/solid reaction represented by Eq. (27), on the other hand, is slow but reversible. The time scale of this process is of the order of hundreds to thousands of seconds, as evidenced by the time required to experimentally attain the equilibrium O/U ratio in oxidizing gases.

The consequences of this difference in time scales of the surface and surface/solid reactions is that the last term in Eq. (36) can be neglected; the surface coverages of $H_2O$ and O are independent of the stoichiometry deviation $x$. If in addition the terms in this equation representing $O_2$ adsorption and desorption are neglected, the surface coverages can be determined by solving Eqs. (28) and (29). In dimensionless terms, the equilibrium coverages are given by

$$\theta_{H_2O} = \frac{\alpha P_W}{1 + \alpha P_W\left(1 + \gamma/\delta P_W^{2/3}\right)}, \quad (40)$$

$$\theta_O = \left(\frac{\gamma}{\delta P_W^{2/3}}\right)\theta_{H_2O}, \quad (41)$$

where the rate constants are scaled to the water desorption rate constant:

$$\gamma = \frac{k_a''}{k_a}, \qquad \alpha = \frac{2\beta_{H_2O}}{K_W k_a n_S}, \qquad \delta = \frac{2k}{K_W k_a}, \quad (42)$$

and $P_W$ is the dimensionless steam pressure:

$$P_W = \tfrac{1}{2} K_W P_{H_2O}. \quad (43)$$

Eq. (38) is written as

$$\frac{dx}{dt} = \frac{1}{t_{char}}\left[\theta_O - E\left(1 - \theta_O - \theta_{H_2O}\right) q(x)\right], \quad (44)$$

where

$$t_{char} = \left(k_s \frac{n_S S}{\rho_U V}\right)^{-1}. \quad (45)$$

The parameter $E$ of Eq. (35) becomes

$$E = \frac{\alpha\gamma}{\delta} = \frac{\alpha P_W\left(\gamma/\delta P_W^{2/3}\right)}{P_W^{1/3}}. \quad (46)$$

To scale the time properly, the initial oxidation rate (when $x = 0$ and the oxygen activity $q$ is very small) is given by Eq. (44) as

$$\left(\frac{dx}{dt}\right)_{t=0} = \frac{\theta_O}{t_{char}}. \quad (47)$$

Model solutions that satisfactorily reproduce experimental data in the form of $x$ vs. $t$ can be constructed from a wide range of the parameters $\alpha P_w$ and $\gamma/\delta P_W^{2/3}$. Given these two quantities, the coverages follow from Eqs. (40) and (41), and the characteristic time is obtained from Eq. (47). Eq. (44) can then be integrated numerically using an appropriate thermochemical model for the oxygen activity function $q(x)$.

To illustrate the application of the model, the following parameter values are arbitrarily chosen for a steam pressure of 1 atm at 1623 K:

$$\alpha P_W = 0.01, \qquad \gamma/\delta P_W^{2/3} = 0.005.$$

Using these values, Eq. (40) gives a water coverage of 0.099 and Eq. (41) yields an O atom coverage of $5.0 \times 10^{-5}$. At 1623 K, the laboratory experiments exhibit an

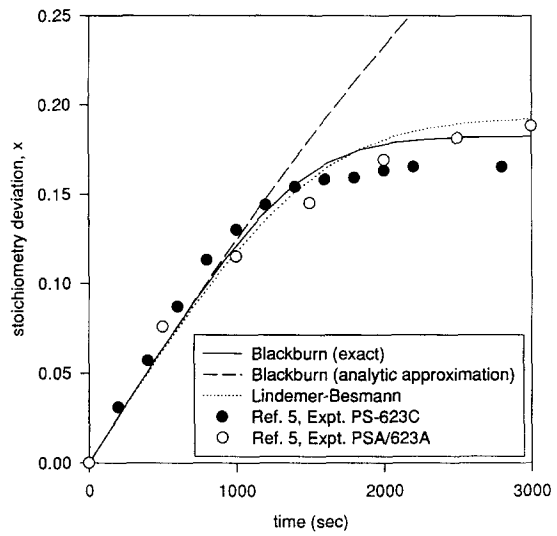


Fig. 3. $UO_2$ oxidation kinetics at 1623 K in pure steam at 1 atm pressure.

initial oxidation rate of $\sim 1.3 \times 10^{-4}$ s$^{-1}$ [5]. At this temperature the dimensionless pressure of Eq. (43) is $P_w = 5 \times 10^9$ for a steam pressure of one atm. Eq. (47) gives $t_{char} = 0.38$ s and from Eq. (46), $E = 2.9 \times 10^{-8}$. From Eq. (44), the final oxygen activity at equilibrium is

$$q(x_{eq}) = \frac{\theta_O}{E(1 - \theta_O - \theta_{H_2O})} \cong 1700.$$

Using Blackburn's full thermochemical model (not its analytic approximation), the stoichiometry deviation corresponding to this oxygen activity is $x_{eq} = 0.18$, which is close to the experimentally-observed value for these conditions.

Fig. 3 shows theoretical oxidation curves for three $UO_{2+x}$ thermochemical models: the full model of Blackburn [11]; the analytic approximation to Blackburn's model:

$$\ln P_{O_2} = 2 \ln\left(\frac{x(2+x)}{1-x}\right) - \frac{32\,900}{T} + 10.2; \qquad (48)$$

and the analytic approximation to the representation of Lindemer and Besmann [12]:

$$P_{O_2} = \min(P_1, P_2),$$

where

$$\ln P_1 = 2 \ln\left(\frac{x(1-2x)^2}{(1-3x)^3}\right) - \frac{37\,620}{T} + 15.15,$$

$$\ln P_2 = 4 \ln\left(2\frac{x(1-2x)}{(1-4x)^2}\right) - \frac{43\,300}{T} + 25.74. \qquad (49)$$

The points in Fig. 3 represent two experimental runs. The agreement between the model and the experiments is well within experimental reproducibility, although the theory appears to slightly overestimate the equilibrium O/U ratio. This is a problem with the $UO_2$ thermochemical model, not with the kinetic model. The full Blackburn model and Lindemer and Besmann's analytical representation are in fair agreement for the particular reaction conditions of Fig. 3. However, this accord does not hold over wide ranges of temperature and oxygen potential. Eq. (48) grossly overestimates the final stoichiometry in Fig. 3, although under other T–O/U combinations, it is a fairly good approximation to Blackburn's exact computation.

The problem of preventing inaccuracies in the thermochemical model from affecting assessment of the kinetic model can be handled easily in the Gala–Grabke approach of Eq. (9) and in Dobrov's theoretical formula of Eq. (22a). In both of these formulations, the thermodynamic limit appears as the simple function $1 - q(x)/(P_{H_2O}/P_{H_2})$. In order to make allowance for an erroneous thermochemical function $q(x)$, the actual oxygen activity of the gas (i.e., the steam-to-hydrogen pressure ratio) is replaced by the oxygen activity $q(x_{eq})$ that gives the final stoichiometry deviation $x_{eq}$ observed in the oxidation kinetic tests. In this way, the effect of inaccuracies in the thermochemical model on kinetic data interpretation are largely removed. This technique was employed in Ref. [5], and although not explicitly stated, appears to have been used by Dobrov et al. [7]. However, this strategy cannot be applied to the more general oxidation model expressed by Eqs. (36)–(38) because the thermochemical limitation does not appear as a simple ratio of $H_2O$ to $H_2$ pressures, as it does in the earlier theories.

The simplified version of the general oxidation model given by Eqs. (40)–(46) contains three kinetic parameters: $\alpha$, $k_s$, and the ratio $\gamma/\delta$. Many combinations of these parameters produce fits to the data as good as that shown in Fig. 3. From the available database, the only guidance to selecting the parameters is correct modeling of the steam-pressure effect on the oxidation rate. Large values of $\alpha P_W$ and $\gamma/\delta P_W^{2/3}$ lead to high coverages and insensitivity of the oxidation rate to steam pressure. Conversely, small values of these parameters lead to low coverages to a significant pressure effect. However, the maximum variation is $P_W^{1/3}$, not the square-root variation that the data very roughly suggest or the Langmuir-type dependence of the model of Dobrov et al. (Eq. (22)).

Fig. 4 compares the present model with the data from an experiment in 0.5 atm steam. The three temperature-dependent kinetic parameters were the same as those used in the 1-atm steam comparison of Fig. 3. Only the $P_W$ variable in Eqs. (40) and (41) was changed. The fit in Fig. 4 is about as good as can be expected given the accuracy of the data. The portion of the database containing steam pressure variations is less extensive than that involving temperature changes. Consequently, it is probably not possible to unequivocally determine whether $\sqrt{P_{H_2O}}$, $P_{H_2O}^{1/3}$, or the Langmuir-type function of Eq. (22a) best represents the effect of steam pressure on oxidation kinetics. More-

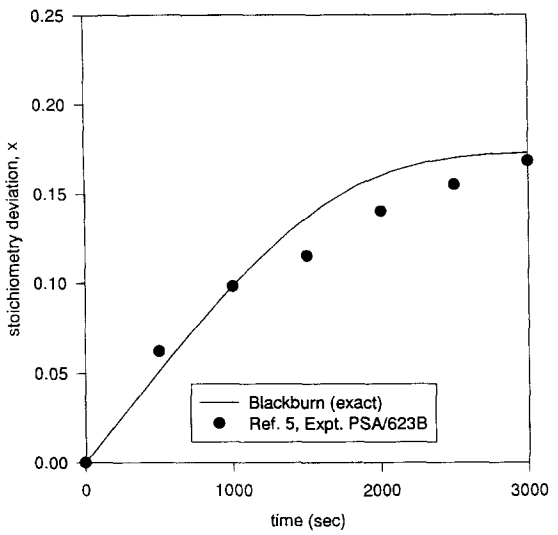


Fig. 4. $UO_2$ oxidation kinetics at 1623 K in pure steam at 0.5 atm pressure.

over, it is unlikely that simple forms apply under all conditions.

The $P_{H_2O}^{1/3}$ dependence predicted from the present model applies only if the reactant gas is pure steam. In this instance, the oxygen pressure is given by Eq. (39), and the $H_2$ pressure is twice this value. These pressures are quite small, being $3 \times 10^{-4}$ and $6 \times 10^{-4}$ atm, respectively, in steam at 1623 K. If the steam is mixed with even a small concentration of $H_2$, the $O_2$ pressure drops by orders of magnitude and the $H_2$ pressure rises by a comparable amount. The pressure effect in this case is (theoretically) very different than that in pure steam: at a constant temperature and $H_2O/H_2$ ratio in the gas, increasing the total pressure decreases rather than increases the initial rate of oxidation. This is because $H_2$ is a scavenger of adsorbed oxygen, and according to Eq. (36), an increase in $P_{H_2}$ reduces the oxygen coverage. The smaller $\theta_O$ in Eq. (38) decreases the oxidation rate. Experimental data are not available to test this prediction.

### 2.7. $H_2O_2(g)$ and OH(ads)

The reaction model given in the preceding section does not include $H_2O_2$ as a reactant gas component. Although experiments have been performed in which this species has been injected into the reactant gas, the reactivity of $H_2O_2$ with apparatus walls and its thermal instability probably cause it to be converted to $H_2O + O_2$ before it reaches the $UO_2$ specimen. In a defective fuel rod operating in a reactor, on the other hand, $H_2O_2$ may be generated in the steam in the fuel-cladding gap and thus be immediately available for reaction with the fuel [2]. To include this species in the mechanism would require adding OH(ads) to the surface-adsorbed population because the primary decomposition step of $H_2O_2(g)$ on the oxide surface is most likely to be

$$H_2O_2(g) \rightarrow 2OH(ads) \tag{50}$$

and additional subsequent elementary steps involving OH(ads) would need to be added to the mechanism. In addition, gas-phase equilibrium could not be assumed because of steam radiolysis by recoiling fission fragments.

### 2.8. Reduction of $UO_{2+x}$ by $H_2$

There is considerable evidence that the reaction of $UO_{2-x}$ with hydrogen (i.e., the reverse step in reactions (13) and (25)) is much faster than oxidation. The oxidation–reduction cycles shown in Ref. [5] exhibit much quicker reduction than oxidation when the ambient gas is switched from steam to hydrogen. Reactions (13) and (25) appear to be so fast that solid-state diffusion of oxygen is the rate-limiting step. Relying on this limiting behavior, Lay [23] measured the oxygen chemical diffusion coefficient in $UO_{2+x}$ between 600° and 1100°C by reduction of hyperstoichiometric specimens in atmospheric-pressure $H_2$.

On the other hand, in a molecular beam experiment at effective gas pressures of $\sim 10^{-7}$ atm, Olander and Dooley [22] found that only the dissociated (atomic) form of hydrogen reduced $UO_{2+x}$ at a detectable rate.

The above observations suggest that subatmospheric pressures will be necessary in order to experimentally measure the surface-reaction kinetics of $UO_{2+x}$ reduction in $H_2$.

### 2.9. Oxidation by $O_2$

Reactions (26) and (27) of the mechanism can be isolated and studied experimentally by using a reactant gas that contains $O_2$ but not $H_2O$. However, to prevent formation of surface layers of $U_4O_9$ or $U_3O_7$, which are known to form in low-temperature oxidation [1], these experiments would have to be conducted at high temperatures and low oxygen partial pressures in an inert carrier gas.

## 3. Conclusions

Mechanistic reaction modeling is required to adequately describe the chemical interactions of $UO_2$ with oxidizing and reducing gases encountered in reactor applications. Existing models are extended within the framework required by the principle of detailed balancing. This principle requires that both forward and reverse reactions of each elementary reaction in the model be included, provides relations between the rate constant and gas–solid thermochemistry, and constrains the forms of the rate laws used to describe the rates of the elementary steps. The importance of judging the physical reasonableness of rate

constants deduced from application of mechanistic models to experimental data is demonstrated.

The extended model contains the minimum set of elementary steps to permit use in interpreting reaction kinetics of future experiments involving $UO_2$. These include reduction in $H_2$ at pressures sufficiently low to avoid solid-state diffusion control, oxidation by $O_2$, and oxidation by steam at pressures greater than one atmosphere. Additional experiments are needed to probe different portions of the reaction mechanism. As new experimental data become available, extension of the reaction model may be necessary to incorporate additional surface species such as OH(ads) and the elementary reactions in which this species is involved.

## Acknowledgements

The helpful comments of Brent Lewis are gratefully acknowledged.

## References

[1] R.J. McEachern, P. Taylor, A review of the oxidation of uranium dioxide at temperatures below 400°C, J. Nucl. Mater., (1998) in press.
[2] D.R. Olander, W.-E. Wang, Y.S. Kim, C. Li, K. Lim, Chemistry of Defective Light-Water Reactor Fuel, Electric Power Research Institute Report TR-107074, Dec. 1996.
[3] J.T. Bittel, L.H. Sjodahl, J.F. White, J. Am. Ceram. Soc. 52 (1969) 446.
[4] D.S. Cox, F.C. Iglesias, C.E.L. Hunt, N.A. Keller, R.D. Barrand, J.R. Mitchell, R.F. O'Connor, Proc. Symp. On Chemical Phenomena Associated with Radioactivity Releases During Severe Nuclear Plant Accidents, Anaheim, CA, NUREG/CP-0078, Sept. 1986, pp. 2-35 to 2-49.
[5] J. Abrefah, A. de Aguiar Braid, W.-E. Wang, Y. Khalil, D.R. Olander, J. Nucl. Mater. 208 (1994) 98.
[6] M. Imamura, K. Une, J. Nucl. Mater. 233 (1995) 40.
[7] B.V. Dobrov, V.V. Likhanskii, V.D. Orzin, A.A. Solodov, M.P. Kissane, H. Manenc, Kinetics of $UO_2$ oxidation in steam atmospheres, J. Nucl. Mater., submitted.
[8] J.J. Katz, E. Rabinowitz, The Chemistry of Uranium, Dover, New York, 1951, p. 309.
[9] Hj. Matzke, J. Chem. Soc. Faraday Trans. 2 (1987) 425.
[10] R.E. Carter, K.W. Lay, J. Nucl. Mater. 36 (1970) 77.
[11] P. Blackburn, J. Nucl. Mater. 46 (1973) 244.
[12] T.B. Lindemer, T.M. Besmann, J. Nucl. Mater. 130 (1985) 473.
[13] T.J. Heames et al., VICTORIA: a Mechanistic Model of Radionuclide Behavior in the Reactor Coolant System Under Severe Accident Conditions, NUREG/CR-5545 Rev. 1, 1992.
[14] W. Yourgrau, A. van der Merwe, G. Raw, Treatise in Irreversible and Statistical Thermophysics, Macmillan, 1982, pp. 24–29.
[15] A. Katchalsky, P.F. Curran, Nonequilibrium Thermodynamics in Biophysics, Harvard University, 1967, pp. 94–97.
[16] A. Gala, H.J. Grabke, Arch. Eisenhuttenw. 43 (1972) 463.
[17] D.O. Hayward, B.M.W. Trapnell, Chemisorption, Butterworth, 1964.
[18] R.C. Baetzold, G.A. Somorjai, J. Catal. 45 (1976) 94.
[19] B.J. Lewis, personal communication, 1997.
[20] R.H. Jones, D.R. Olander, W.J. Siekhaus, J.A. Schwarz, J. Vac. Sci. Technol. 9 (1972) 1429.
[21] A.J. Machiels, D.R. Olander, High Temp. Sci. 9 (1977) 3.
[22] D.R. Olander, D.F. Dooley, J. Nucl. Mater. 139 (1986) 237.
[23] K.W. Lay, J. Am. Ceram. Soc. 53 (1970) 369.